Biosensors and Bioelectronics 126 (2019) 493–500

Contents lists available at ScienceDirect

Biosensors and Bioelectronics

journal homepage: www.elsevier.com/locate/bios

An electrochemical immunobiosensor for ultrasensitive detection of *Escherichia coli* O157:H7 using CdS quantum dots-encapsulated metal-organic frameworks as signal-amplifying tags

Miao Zhong, Lu Yang, Hui Yang, Chang Cheng, Wenfang Deng, Yueming Tan*, Qingji Xie, Shouzhuo Yao

Key Laboratory of Chemical Biology and Traditional Chinese Medicine Research (Ministry of Education of China), College of Chemistry and Chemical Engineering, Hunan Normal University, Changsha 410081, China

ARTICLE INFO

Keywords:
Metal-organic frameworks
CdS quantum dot
Immunobiosensor
Escherichia coli O157:H7
Zeolitic imidazolate framework-8

ABSTRACT

We report here cadmium sulfide quantum dots (CdS QDs)-encapsulated metal-organic frameworks as signal-amplifying tags for ultrasensitive electrochemical detection of *Escherichia coli* O157:H7 (*E. coli* O157:H7). CdS QDs were encapsulated in zeolitic imidazolate framework-8 (ZIF-8) to form CdS@ZIF-8 muti-core-shell particles by in situ growth of ZIF-8 in the presence of CdS QDs. To specifically recognize *E. coli* O157:H7 cells, CdS@ZIF-8 particles were coated with polyethyleneimine to introduce amino groups on their surfaces, followed by surface modification of anti-*E. coli* O157:H7 antibody. A sandwich-type electrochemical immunobiosensor for the detection of *E. coli* O157:H7 was fabricated using CdS@ZIF-8 particles as signal tags. Cd(II) ions were released from CdS@ZIF-8 tags by HCl leaching, enabling the detection of *E. coli* O157:H7 by differential pulse voltammetry. Under the optimized conditions, the linear range of the biosensor is from 10 to 10^8 colony forming units (CFU) per mL for *E. coli* O157:H7 detection, with the detection limit of 3 CFU mL^{-1} ($S/N = 3$). The sensitivity of the biosensor for *E. coli* O157:H7 detection using CdS@ZIF-8 particles as signal tags is 16 times that of a biosensor using CdS QDs as signal tags, because the number of CdS QDs labeled to each bacterial cell increases greatly resulting from a great number of CdS QDs encapsulated in each CdS@ZIF-8 label. This method was successfully used to detect *E. coli* O157:H7 in milk samples.

1. Introduction

Foodborne illnesses mainly caused by pathogenic bacteria have become a global concern of food safety problems (Mead et al., 1999). For preventing and controlling foodborne illnesses, rapid and accurate detection of foodborne pathogenic bacteria is important (Alocilja and Radke, 2003). Conventional culture-based methods are considered as the "gold standard" for the detection pathogenic bacteria, but they have the disadvantage of long detection cycle (Deisingh and Thompson, 2004). Some modern detection technologies, such as immunology-based enzyme linked immunosorbent assay, polymerase chain reaction technologies, DNA probe technique, gene hcip technology, have been adopted for the detection of pathogenic bacteria (Anderson et al., 2013; Atrazhev et al., 2010; Charlermroj et al., 2013; Fortin et al., 2001; Mao et al., 2006; Sun et al., 2015; Thaitrong et al., 2013). Although these methods can show good specificity and high sensitivity for pathogen detection, some shortcomings including high cost, high technical requirements, and complicated detection procedures still retard their wide applications.

Various biosensors based on biological recognition technologies (e.g., immunological recognition) have been reported for the detection of pathogenic bacteria (Gayathri et al., 2016; Salam et al., 2013; Santos et al., 2013; Setterington and Alocilja, 2011; Shen et al., 2007; Su and Li, 2004; Wang et al., 2017a, 2017b; Wu et al., 2014; Xu et al., 2017; Yang et al., 2018, 2004; Zhang et al., 2016). Especially, electrochemical biosensors have been widely used for detection of pathogens, owing to their advantages including fast analysis speed, low cost, simple instrumentation, ease of miniaturization, and suitability for on-site detection (Gayathri et al., 2016; Santos et al., 2013; Setterington and Alocilja, 2011; Wang et al., 2017a; Xu et al., 2017; Yang et al., 2004; Zhang et al., 2016). For instance, a label-free electrochemical impedimetric immunosensor has been reported for the detection of *Escherichia coli* O157:H7 (*E. coli* O157:H7), showing a detection limit of 10^6 colony forming units per mL (CFU mL^{-1}) (Yang et al., 2004). The binding of

* Corresponding author.
E-mail address: tanyueming0813@hunnu.edu.cn (Y. Tan).

https://doi.org/10.1016/j.bios.2018.11.001
Received 16 July 2018; Received in revised form 31 October 2018; Accepted 1 November 2018
Available online 02 November 2018
0956-5663/

bacterial cells to electrode via immunological recognition can result in the increase of electron-transfer resistance, so *E. coli* O157:H7 can be simply detected by impedance spectroscopy (Yang et al., 2004). Compared with impedimetric biosensors, amperometric biosensors using electroactive molecules, enzymes, and nanomaterials as electrochemical labels usually have higher sensitivities (Setterington and Alocilja, 2011; Zhang et al., 2016). For instance, a sandwich-type amperometric immunosensor for the detection of pathogenic bacteria has been reported using multiwalled carbon nanotubes (MWCNTs)-horseradish peroxidase (HRP) nanocomposites as labels, showing a detection limit of 50 CFU mL^{-1} (Zhang et al., 2016). HRP loaded on MWCNTs can catalyze the oxidation of aniline to produce polyaniline, so pathogenic bacteria can be quantitatively detected by measuring the oxidation current of polyaniline (Zhang et al., 2016). However, the detection limits of most biosensors reported previously ranged from 10^2 to 10^5 of CFU mL^{-1} for the detection of pathogenic bacteria (Gayathri et al., 2016; Santos et al., 2013; Wang et al., 2017a; Xu et al., 2017; Yang et al., 2004; Zhang et al., 2016), which are still difficult to meet the requirements of practical applications, because the infectious doses of many pathogenic bacteria (e.g., *E. coli* O157:H7) are usually as low as 10 cells. Therefore, it is still urgent to develop an effective signal amplification strategy to further improve the sensitivity of biosensors.

Metal organic frameworks (MOFs) consisting of inorganic metal ions/clusters and organic ligands, have ultrahigh porosity and large surface areas (Lee et al., 2009; Ling et al., 2015; Ma et al., 2013; Shen et al., 2015; Wang and Cohen, 2009). Recently, the encapsulation of nanomaterials in MOFs to form composite materials has raised special concerns, because the composite materials can show superior properties to those of the individual components for various applications (Chen et al., 2017; Zhu and Xu, 2014). Quantum dots (QDs) with unique optical and electrical properties, have been used in a wide range of fields, including solar photon conversion, photocatalysis, optical sensors, and biological imaging (Alivisatos, 1996; Dutta and Kumar, 2016; Hildebrandt et al., 2017; Kokkinos et al., 2016; Michalet et al., 2005). To improve the stability and modulate the optical properties of QDs, various QDs have been encapsulated in MOFs (Aguilera-Sigalat and Bradshaw, 2016; Buso et al., 2012; Esken et al., 2011; Saha et al., 2014; Zhan et al., 2013). In recent years, the optical properties of QDs-encapsulated MOFs have been studied intensively, but the electrochemical application of QDs-encapsulated MOFs has scarcely been exploited.

Herein, CdS QDs encapsulated zeolitic imidazolate framework-8 (ZIF-8) particles were prepared and used as signal-amplifying tags for ultrasensitive electrochemical detection of *E. coli* O157:H7. CdS@ZIF-8 muti-core-shell particles were prepared by in situ growth of ZIF-8 in the presence of CdS QDs. A great number of CdS QDs were encapsulated in each ZIF-8 nanoparticle, which was confirmed by transmission electron microscopy (TEM), energy dispersive X-ray (EDX) elemental mapping, and atomic absorption spectrometry (AAS). After surface coating of polyethyleneimine (PEI) and further modification of anti-*E. coli* O157:H7 antibody (Ab), the CdS@ZIF-8 particles can specifically recognize *E. coli* O157:H7 cells, so a sandwich-type electrochemical immunobiosensor was fabricated using CdS@ZIF-8 particles as signal tags. The CdS@ZIF-8 tags can be dissolved by HCl leaching, and Cd(II) ions were released, enabling the detection of *E. coli* O157:H7 by differential pulse voltammetry (DPV). Because a great number of CdS QDs were encapsulated in each CdS@ZIF-8 label, the number of CdS QDs labeled to each bacterial cell increased greatly. As a result, the electrochemical signals were amplified greatly by using CdS@ZIF-8 particles as signal tags.

2. Experimental

2.1. Instrumentation and reagents

TEM images were obtained with a Philips TECNAI F-30 transmission electron microscope. Scanning electron microscopy (SEM) images were obtained with a JSM-6360 field emission scanning electron microscope. Fourier transform infrared (FTIR) spectra were collected on Nicolet Nexus 670 Fourier transform infrared spectrometer. AAS measurements were carried out on a WFX-110A Atomic Absorption Spectrophotometer. All electrochemical experiments were performed on a CHI760E electrochemical workstation in a three-electrode system. The three-electrode system consists of a modified glassy carbon electrode (GCE, diameter 3 mm) as the working electrode (WE), a KCl-saturated calomel electrode (SCE) as the reference electrode (RE), and a Pt wire (diameter 0.1 mm) as the counter electrode (CE).

All reagents were analytical grade and without further purification. Cadmium chloride ($CdCl_2{\cdot}2.5H_2O$), Sodium sulfide ($Na_2S{\cdot}9H_2O$) were purchased from Damao Chemical Reagent Factory (Tianjin, China). Mercaptoacetic acid, sodium hydroxide, hydrochloric acid, ethanol, 2-Methylimidazole were purchased from Sinopharm Chemical Reagent Co. Ltd. (Shanghai, China). Zinc acetate ($Zn(Ac)_2{\cdot}H_2O$) was purchased from Kermel Chemical Reagent Co., Ltd. (Shanghai, China). *P*-aminobenzoic acid was purchased from Tianjin Guangfu Fine Chemical Research Institute. 1-(3-(dimethylamino)-propyl) − 3-ethylcarbodiimide hydrochloride (EDC), N-hydroxysuccinimide (NHS), bovine serum albumin (BSA) were purchased from Sigma Aldrich. PEI was purchased from Aladdin. The Rabbit Anti-*E.coli O157:H7* Ab was purchased from Beijing Biosynth. Biotechnol. Co. Ltd. (Beijing, China). The washing and blocking buffer solution for immunoassay was 0.1 M PBS (pH 7.4, 10 mM NaH_2PO_4-Na_2HPO_4 + 0.15 M NaCl). Milli-Q ultrapure water (Millipore, ≥ 18 MΩ cm) was used throughout.

2.2. Preparation of CdS QDs and CdS@ZIF-8 particles

CdS QDs were prepared following the reported synthesis strategy (Dutta and Kumar, 2016). Briefly, a pure mercaptoacetic acid liquid was added dropwise to 25 mL of 0.01 M aqueous $CdCl_2$ under vigorous stirring condition until the solution pH changed to 2.0. After stirring for another 30 min, 1 M aqueous NaOH was added dropwise to the above solution under vigorous stirring condition until the solution pH changed to 6.0. 25 mL of 5 mM aqueous Na_2S was added dropwise to the above solution under vigorous stirring condition and the mixture was continuously stirred for 1 h. Finally, The CdS QDs precipitated with ethanol were collected by centrifugation, washed with ethanol-water solution for several times and finally dried in a vacuum freeze dryer.

For the preparation of CdS@ZIF-8 particles, 15 mg of CdS QDs were ultrasonically dispersed in 3 mL of 1.6 M 2-methylimidazole aqueous solution. Then 0.8 mL of 0.3 M zinc acetate aqueous solution was added to the above solution. After 30 min reaction, the products of CdS@ZIF-8 particles were collected by centrifugation at 5000 rpm, washed with water, and finally dried in a vacuum freeze dryer.

2.3. Preparation of Ab-conjugated CdS@ZIF-8 particles and Ab-conjugated CdS QDs

To introduce amino groups on the surfaces of CdS@ZIF-8 particles, CdS@ZIF-8@PEI particles were prepared as follows. 200 μL of 0.1 M PBS (pH 7.4) containing 1 wt% PEI was added into 1 mL of PBS containing 2 mg mL^{-1} CdS@ZIF-8. The mixture was continuously stirred for 1 h, and CdS@ZIF-8@PEI particles were obtained.

Ab-conjugated CdS@ZIF-8 particles were prepared as follows. The CdS@ZIF-8@PEI particles were collected by centrifugation, washed with PBS, and dispersed in 1 mL of PBS containing 0.25 wt% glutaraldehyde. After reaction for 30 min, the products were collected by centrifugation, washed with PBS, and dispersed in 0.5 mL PBS. Then 0.5 mL of PBS containing anti-*E. coli* O157:H7 Ab (1 mg mL^{-1}) was mixed with the above dispersion. After reaction for 2 h (Ab incubation), the products denoted as CdS@ZIF-8@PEI-Ab were collected by centrifugation, washed with PBS, and dispersed in 0.5 mL of PBS containing 1 wt% BSA. After gentle agitation for 30 min, the CdS@ZIF-8@PEI-Ab particles blocked by BSA were collected by centrifugation,

washed with PBS, and dispersed in 0.5 mL of PBS, stored at 4 °C for future use.

Mercaptoacetic acid is capped on CdS QDs, enabling facile modification of anti-*E. coli* O157:H7 Ab on CdS QDs. Ab-conjugated CdS QDs were prepared as follows. 2 mg of CdS QDs were dispersed in 1 mL of PBS containing 400 mM EDC and 100 mM NHS. After vigorous shaking for 1 h, then the mixture was centrifuged, washed with PBS, and dispersed in 1 mL of PBS containing 100 μg mL^{-1} anti-*E. coli* O157:H7 Ab. After vigorous shaking for another 6 h (Ab incubation), Ab-conjugated CdS QDs were collected by centrifugation, washed with PBS, and dispersed in 1 mL of PBS containing 1 wt% BSA. After gentle agitation for 30 min, Ab-conjugated CdS QDs blocked by BSA were collected by centrifugation, washed with PBS, and dispersed in 1 mL of PBS, stored at 4 °C for future use.

Sodium dodecyl sulfate polyacrylamide gel electrophoresis (SDS-PAGE) was carried out to confirm the successful modification of anti-*E. coli* O157:H7 Ab on the surfaces of various samples. In the experiment, 2 μL of sample was mixed with 8 μL of Milli-Q water and 2 μL of 6 × loading buffer, and then the mixture was loaded into SDS-PAGE gel. A 0.5 M Tris/boric acid buffer was used as the running buffer. The gel was run for 1 h at a voltage of 120 V.

2.4. Bacterial growth

E. coli O157:H7, *E. coli* K12, and *S. aureus* grew in sterile Luria-Bertani (LB) media (2.0 g bacto-tryptone, 1.0 g bacto-yeast extract powder, 2.0 g NaCl dissolving in 200 mL distilled water, and adjusted to pH 7.4 with 3.0 M NaOH) in an incubator-shaker at 37 °C to reach the growing stationary phase. After overnight incubation, 1 mL of bacterial cells was centrifuged (6000 rpm, 10 min) to remove the supernatant and washed 3 times with PBS (0.1 M, pH 7.4), and resuspended in 1 mL of PBS. Howbeit, *L. monocytogenes* grew in Nutrient-Broth (NB) media (2.0 g bacto-peptone, 0.6 g bacto-beef extract, 1.0 g NaCl dissolving in 200 mL distilled water, and adjusted to pH 7.4 with 3.0 M NaOH). By plating bacteria on LB or NB plates, the amount of bacteria per milliliter can be acquired by counting related colony forming units (CFU) after incubation overnight at 37 °C.

2.5. Fabrication of electrochemical immunobiosensors

The fabrication steps of the immunobiosensor using CdS@ZIF-8 particles as signal tags are shown in Fig. 1**a**. Poly(*p*-aminobenzoic acid) (PABA) modified GCE, diameter 3 mm was prepared by potential cycling between 0.40 V and 1.20 V at 10 mV s^{-1} for 2 cycles in PBS containing 10 mM KCl and 1.0 mM *p*-aminobenzoic acid (Fig. S1). To activate the carboxylic groups on PABA, the PABA/GCE electrode was soaked in PBS containing 100 mg mL^{-1} EDC and 100 mg mL^{-1} NHS for 30 min. Then 10 μL of PBS containing 0.1 mg mL^{-1} anti-*E.coli* O157:H7 Ab was dropped on the activated PABA/GCE and kept at 37 °C for 1 h to immobilize anti-*E.coli* O157:H7 Ab, and the excess Ab molecules was washed away with PBS. The resulting electrode was denoted as Ab-PABA/GCE. To block the nonspecific binding sites, the Ab-PABA/GCE was immersed in PBS containing 1 wt% BSA at 37 °C for 0.5 h, and the resulting electrode was denoted as BSA/Ab-PABA/GCE. After washing with PBS, the BSA/Ab-PABA/GCE was incubated in 1 mL of PBS containing different concentrations of *E. coli* O157:H7 cells (the exact concentration was determined by the traditional plate-counting method) at 37 °C for 1 h to form *E. coli* O157:H7/BSA/Ab-PABA/GCE. Subsequently, the *E. coli* O157:H7/BSA/Ab-ABA/GCE was incubated in 0.5 mL of PBS containing 4 mg mL^{-1} CdS@ZIF-8@PEI-Ab at 37 °C for 1 h to form CdS@ZIF-8@PEI-Ab/*E. coli* O157:H7/BSA/Ab-PABA/GCE. The fabrication steps of an immunobiosensor using CdS QDs as signal tags were similar to those of the immunobiosensor using CdS@ZIF-8 as signal tags except that Ab-modified CdS QDs were used instead of CdS@ZIF-8@PEI-Ab.

2.6. Electrochemical measurements

The immunoelectrodes at different fabrication steps were characterized by cyclic voltammetry and electrochemical impedance spectroscopy using 5.0 mM $[Fe(CN)_6]^{4-/3-}$ as the probe. Cyclic voltammograms were recorded at a scan rate of 50 mV s^{-1} in the potential range between −0.2 V and 0.6 V. Electrochemical impedance spectroscopy was performed at an AC voltage amplitude of 5 mV in the frequency range from 1 MHz to to 0.01 Hz. As illustrated in Fig. 1**b**, DPV was carried out to quantitatively detect *E. coli* O157:H7. 5 μL of 0.1 mol L^{-1} HCl aqueous solution was dropped on the immunoelectrode electrode for 5 min to release Cd(II) ions from the tags, followed by adding 15 μL of 0.20 M acetate buffer (pH 4.5) to the immunoelectrode electrode. Then a deposition potential of − 1.0 V and a deposition time of 60 s were applied to the immunoelectrode electrode. Differential pulse stripping voltammograms were recorded between − 1.0 V and −0.4 V, with pulse amplitude of 50 mV and pulse frequency of 15 Hz. As proven by our recent works (Qin et al., 2015, 2016), DPV carried out in small volume of electrolyte solution can greatly enhance electrochemical signals due to the efficient capture of Cd(II) ions from electrolyte solution.

3. Results and discussion

3.1. Synthesis and characterizations of CdS QDs and CdS@ZIF-8 particles

CdS QDs were prepared using mercaptoacetic acid as capping agent. The TEM image in Fig. S2a reveals the formation of monodispersed spherical particles with an average diameter of 3 nm. The high-resolution TEM (HRTEM) image in Fig. S2b shows clear lattice fringes, indicating that CdS QDs are highly crystalline. The lattice spacing is 0.335 nm, corresponding to the (111) plane of cubic CdS. The presence of mercaptoacetic acid on the surfaces of CdS QDs was confirmed by FTIR spectroscopy. As shown in Fig. S2c, the FTIR shows two absorption peaks associated with symmetric stretching vibration (1385 cm^{-1}) and asymmetric stretching vibration (1576 cm^{-1}) of carboxylate groups, indicating the presence of mercaptoacetic acid on the surfaces of CdS QDs.

CdS QDs were encapsulated in ZIF-8 to form core-shell CdS@ZIF-8 particles. CdS@ZIF-8 particles were prepared by in situ growth of ZIF-8 in the presence of CdS QDs. As illustrated in Fig. S3, both COOH groups on the surfaces of CdS QDs and 2-methylimidazole can coordinate with Zn(II) ions, enabling the encapsulation of CdS in ZIF-8 particles. The size and shape of CdS@ZIF-8 particles were characterized by SEM and TEM, revealing that CdS@ZIF-8 particles have a regular rhombic dodecahedron shape (Fig. 2**a**). The average diameter of CdS@ZIF-8 is ca. 670 nm (Fig. 2**b**). The HRTEM image of CdS@ZIF-8 in Fig. 2**c** shows clear lattice fringes of CdS, confirming that CdS QDs were successfully encapsulated in ZIF-8 particles. EDX elemental mapping analysis result in Fig. 2**d** shows that C, N, Zn, Cd, and S are uniformly distributed in ZIF-8 particles, verifying that a great number of CdS QDs are encapsulated in ZIF-8 particles. The density of CdS@ZIF-8 was measured to be 1.1 g cm^{-3}, which is higher than that of pure ZIF-8 (0.95 g cm^{-3}) (Tan et al., 2010). The content of Cd in CdS@ZIF-8 quantitatively measured by AAS is 8.83 wt%. The high Cd content further indicates that a great number of CdS QDs are encapsulated in ZIF-8 particles. The number of CdS QDs in each CdS@ZIF-8 particle can be estimated according to the following equation: $\rho_1 V_1 w = \rho_2 V_2 n$, where ρ_1 is the density of CdS@ZIF-8 (1.1 g cm^{-3}), V_1 is volume of CdS@ZIF-8 (diameter: 670 nm), w is the content CdS (11.3 wt%), ρ_2 is the density of CdS QDs (4.82 g cm^{-3}), V_2 is the density of CdS QDs (diameter: 3 nm), and n is the number of CdS QDs in each CdS@ZIF-8 particle. Thus we can conclude that each CdS@ZIF-8 particle contains 2.87 × 10^6 CdS QDs.

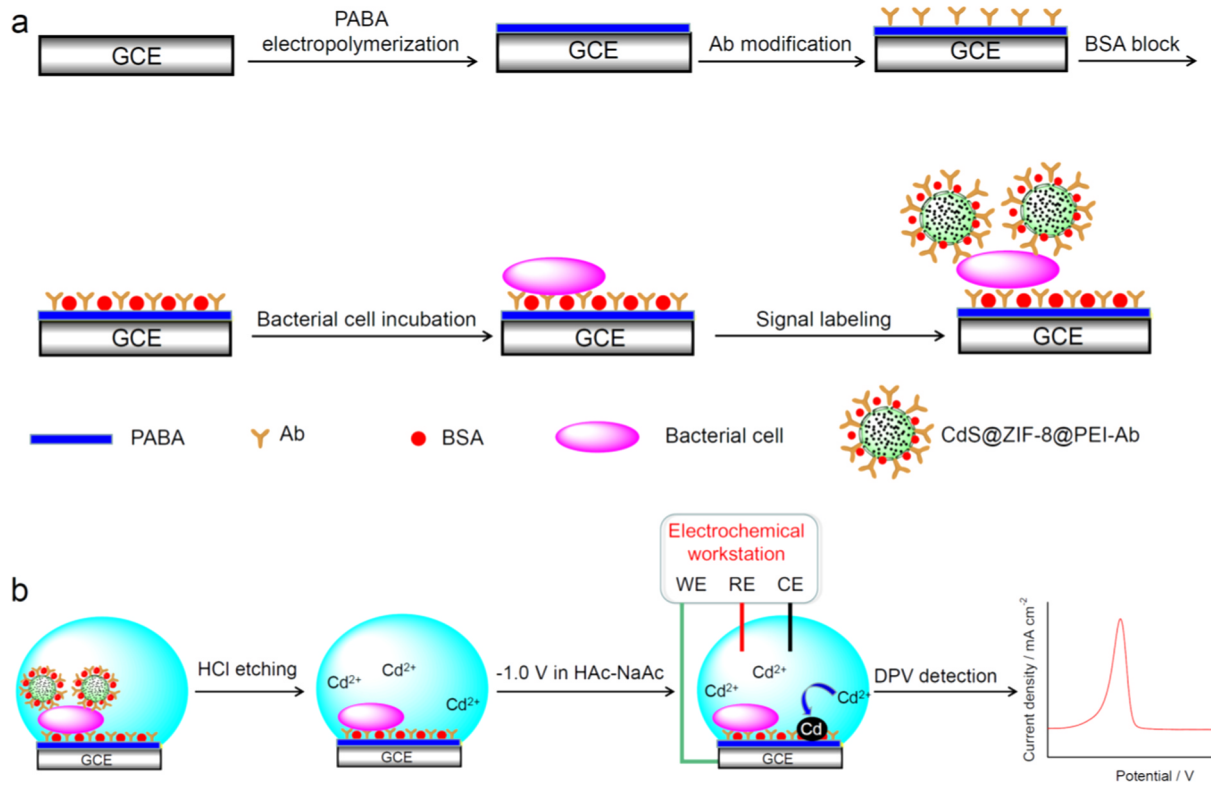

Fig. 1. (a) Schematic illustration of the fabrication steps of the sandwich-type electrochemical immunobiosensor for the detection of *E. coli* O157:H7 using CdS@ZIF-8 as signal tags. (b) Schematic illustration of the steps for DPV detection.

3.2. Surface modifications of CdS@ZIF-8 particles

For covalent immobilization of anti-*E. coli* O157:H7 Ab molecules, CdS@ZIF-8 particles was coated with PEI to introduce amino groups on their surfaces. Fig. S4a shows FTIR spectra of CdS@ZIF-8 before and after surface coating of PEI. The FTIR spectrum of CdS@ZIF-8 shows a sharp absorption peak at 420 nm, which is associated with the Zn-N stretch mode (He et al., 2014). Several absorption bands are also observed at 1300–1500 cm^{-1}, which is assigned to stretching vibration of imidazole ring (Hu et al., 2011). In the FTIR spectrum of PEI, two characteristic peaks at 1578 and 3420 cm^{-1} are attributed to bending vibration and stretching vibration of -NH_2 groups, respectively. An absorption peak is also observed at 1118 cm^{-1}, which corresponds to stretching vibration of C-N bonds. After surface coating of PEI, the resulting CdS@ZIF-8@PEI shows characteristic peaks of NH_2 groups at 1579 and 3425 cm^{-1}, confirming that PEI is successfully coated on

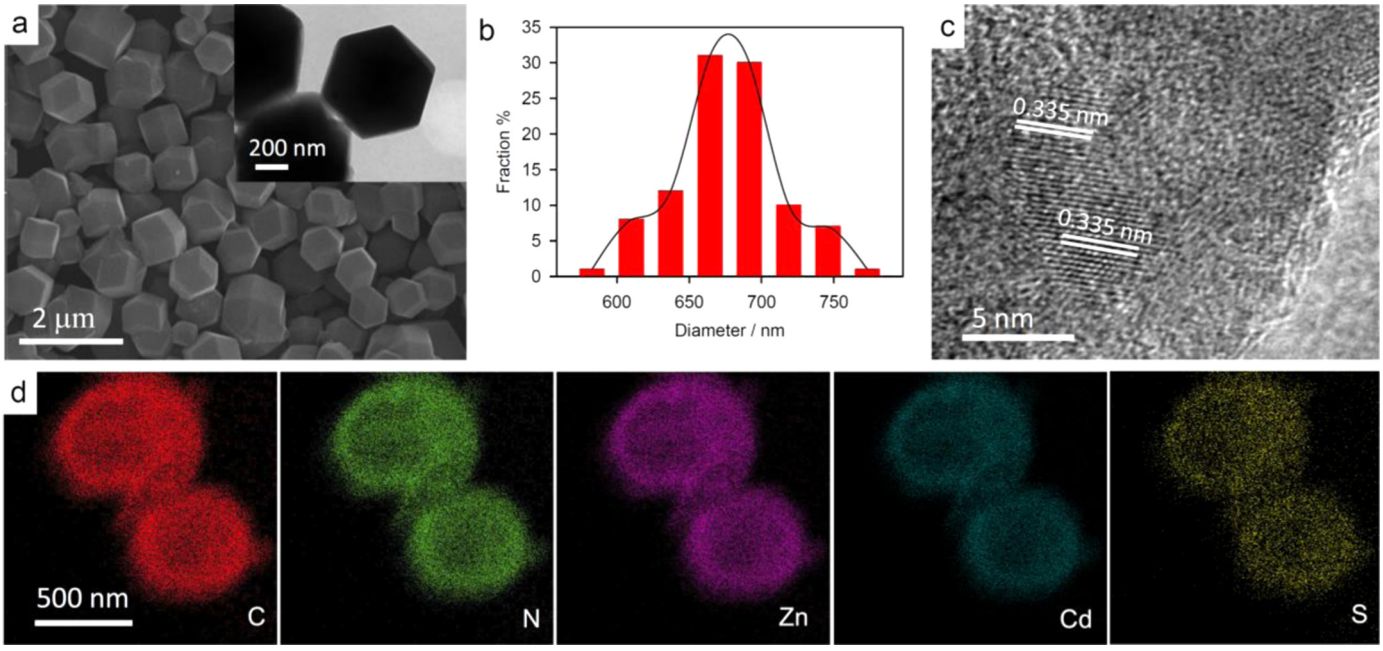

Fig. 2. SEM image (a), TEM image (inset of a), size distribution (b), HRTEM image (c), and EDX elemental mapping (d) of CdS@ZIF-8 particles.

CdS@ZIF-8 particles. The morphology of CdS@ZIF-8@PEI was characterized by SEM. As shown in Fig. S4b, CdS@ZIF-8@PEI particles have approximately spherical shape, which is different from the regular rhombic dodecahedron shape of CdS@ZIF-8 particles. The average diameter of CdS@ZIF-8@PEI particles is ca. 700 nm, which is a little bigger than that of CdS@ZIF-8 particles.

To specially recognize *E. coli* O157:H7 cells, CdS@ZIF-8@PEI particles were conjugated with anti-*E. coli* O157:H7 Ab. To confirm the successful immobilization of anti-*E. coli* O157:H7 Ab molecules on CdS@ZIF-8@PEI particles, SDS-PAGE was carried out, and the SDS-PAGE results are shown in Fig. S4c. The anti-*E. coli* O157:H7 Ab was used as a reference, which shows a band at approximately 50–60 kDa (Lane 2). Ab-conjugated CdS@ZIF-8@PEI shows a band at approximately 90–100 kDa (Lane 4), while Ab-conjugated CdS QDs show a band at approximately 60–70 kDa. The electrophoretic mobility of Ab-conjugated CdS@ZIF-8@PEI and Ab-conjugated CdS QDs is lower than that of Ab alone, confirming the successful immobilization of anti-*E. coli* O157:H7 Ab on CdS@ZIF-8@PEI particles and CdS QDs.

3.3. Fabrication and characterizations of immunoelectrodes

An immunobiosensor for the detection of *E. coli* O157:H7 was fabricated using CdS@ZIF-8@PEI-Ab particles as signal tags. The fabrication steps are illustrated in Fig. 1**a**. The immunoelectrodes at different fabrication steps were characterized by cyclic voltammetry and electrochemical impedance spectroscopy using $[Fe(CN)_6]^{4-/3-}$ as the probe (Fig. 3). A pair of reversible redox peaks for redox of $[Fe(CN)_6]^{4-/3-}$ was observed in the voltammogram in Fig. 3**a** at bare GCE with a redox peak separation (ΔE) of 62 mV. A small semicircle was observed in the electrochemical impedance spectrum in Fig. 3**b**, and the charge transfer resistance (R_{ct}) is estimated to be 24.8 Ω by fitting the electrochemical impedance spectrum to the Randles equivalent circuit. The small values of ΔE and R_{ct} indicate a rapid redox process of $[Fe(CN)_6]^{4-/3-}$ at bare GCE. For the facile immobilization of anti-*E. coli* O157:H7 Ab molecules on GCE, PABA/GCE was prepare to introduce –COOH groups on electrode surface. The values of ΔE and R_{ct} for PABA/GCE are 131 mV and 685 Ω, respectively. The greatly increased ΔE and R_{ct} for PABA/GCE compared with those for bare GCE, indicates the successful modification of PABA. For the efficient capture of *E. coli* O157:H7 cells, Ab-PABA/GCE was prepared, which shows a further increased ΔE (153 mV) and R_{ct} (1300 Ω). To block the nonspecific binding sites, BSA/Ab-PABA/GCE was prepared. The values of ΔE and R_{ct} of the resulting BSA/Ab-PABA/GCE are 193 mV and 1823 Ω, respectively.

To specifically capture *E. coli* O157:H7 Ab cells, the BSA/Ab-PABA/GCE was incubated in 1 mL of PBS containing different concentrations of *E. coli* O157:H7 cells at 37 °C for 1 h. The resulting *E. coli* O157:H7/BSA/Ab-PABA/GCE was also characterized by cyclic voltammetry and electrochemical impedance spectroscopy in 0.10 M PBS (pH 7.4) containing 5.0 mM $K_3Fe(CN)_6$ and 5.0 mM $K_4Fe(CN)_6$. For instance, after the incubation in PBS containing 10^4 CFU mL^{-1} *E. coli* O157:H7 cells, the *E. coli* O157:H7/BSA/Ab-PABA/GCE shows a ΔE of 265 mV and a R_{ct} of 2630 Ω (Fig. 3). Finally, the *E. coli* O157:H7/BSA/Ab-PABA/GCE CdS@ZIF-8@PEI-Ab was labeled with CdS@ZIF-8@PEI-Ab to form CdS@ZIF-8@PEI-Ab/*E. coli* O157:H7/BSA/Ab-PABA/GCE, which shows a ΔE of 333 mV and a R_{ct} of 2884 Ω (Fig. 3).

The immunoelectrodes at different fabrication steps were also characterized by SEM. The bare GCE shows a smooth surface (Fig. S5a), while the PABA/GCE has an uneven surface (Fig. S5b). Some aggregates are observed at Ab-PABA/GCE (Fig. S5c) and BSA/Ab-PABA/GCE (Fig. S5d). We can see rod-shaped *E. coli* O157:H7 cell at *E. coli* O157:H7/BSA/Ab-PABA/GCE (Fig. S5e). As shown in Fig. S5f, several CdS@ZIF-8@PEI-Ab particles linked to *E. coli* O157:H7 cell can be observed at CdS@ZIF-8@PEI-Ab/*E. coli* O157:H7/BSA/Ab-PABA/GCE. As estimated above, each CdS@ZIF-8 particle contains 2.87×10^6 CdS QDs, and these CdS QDs can almost cover the whole surface of a bacterial cell. Thus we can anticipate that the immunobiosensor using CdS@ZIF-8 as signal tags will have improved sensitivity compared with the immunobiosensor using CdS QDs as signal tags, though only several CdS@ZIF-8@PEI-Ab particles are labeled to each bacterial cell.

3.4. Electrochemical detection of E. coli O157:H7

E. coli O157:H7 was quantitatively detected by DPV. As shown in Fig. 1**b**, the CdS@ZIF-8@PEI-Ab labeled to bacterial cells was subjected to HCl etching to release Cd(II) ions, and then *E. coli* O157:H7 can be quantified by DPV analysis of Cd(II) ions. Note that here the sensing architecture cannot be fully removed by HCl treatment, but the the residues on the immunoelectrode have no obvious adverse effect on the DPV measurements (Fig. S6). To achieve the highest current response, the experiment conditions were optimized. The optimal incubation time for *E. coli* O157:H7 capture is 60 min (Fig. S7a), and the optimal incubation time for CdS@ZIF-8@PEI-Ab labeling is 60 min (Fig. S7b). The optimal HCl leaching time is 5 min (Fig. S7c). The optimal potential for Cd(II) deposition is − 1.0 V (Fig. S8a), and the optimal deposition time is 60 s (Fig. S8b). The optimal solution pH for DPV measurements is 4.5 (Fig. S8c).

Fig. 4**a** shows differential pulse voltammograms for the detection of *E. coli* O157:H7 using CdS@ZIF-8 particles as signal tags. The DPV measurements were carried out in air atmosphere. As shown in Fig. S9, the presence of O_2 can cause obvious background current at potentials

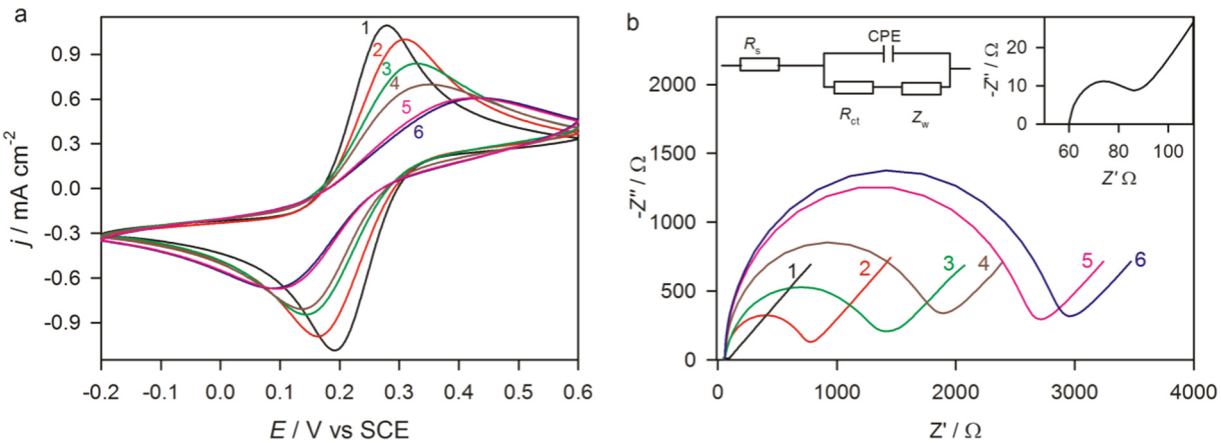

Fig. 3. Cyclic voltammograms (a) and electrochemical impedance spectra (b) of bare GCE (1), PABA/GCE (2), Ab-PABA/GCE (3), BSA/Ab-PABA/GCE (4), *E. coli* O157:H7/BSA/Ab-PABA/GCE (5), and CdS@ZIF-8@PEI-Ab/*E. coli* O157:H7/BSA/Ab-PABA/GCE (6) in 0.10 M PBS (pH 7.4) containing 5.0 mM $K_3Fe(CN)_6$ and 5.0 mM $K_4Fe(CN)_6$. Inset of b shows electrochemical impedance spectrum of bare GCE and equivalent circuit model.

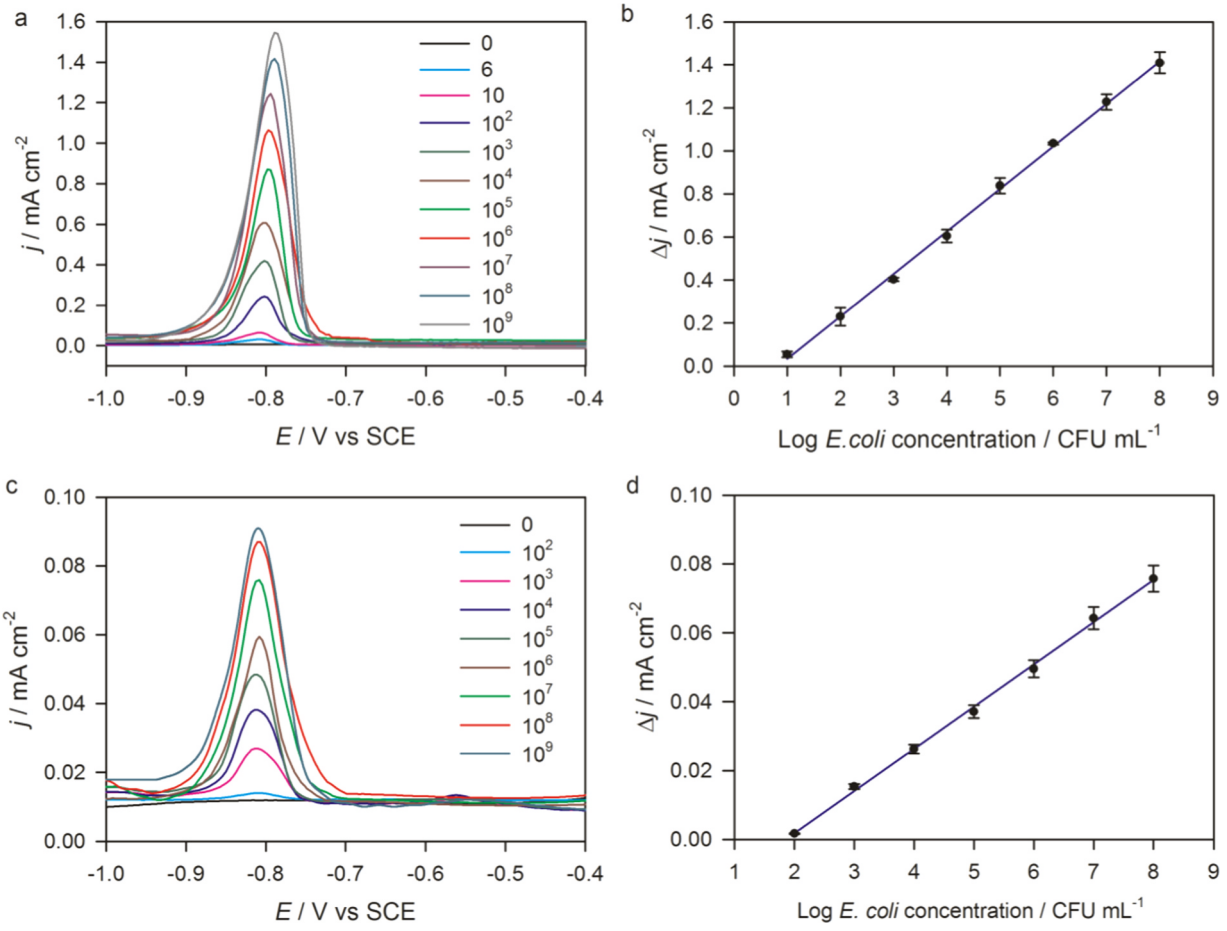

Fig. 4. Differential pulse voltammograms (a) and standard curve (b) for the detection of *E. coli* O157:H7 using CdS@ZIF-8 particles as signal tags. Differential pulse voltammograms (c) and standard curve (d) for the detection of *E. coli* O157:H7 using CdS QDs as signal tags.

below −0.6 V. However, the background currents for various immunoelectrodes are comparable (Fig. 4a), so the electrochemical detection in air atmosphere is feasible. As shown in Fig. 4**a**, even at *E. coli* O157:H7 concentration as low as 6 CFU mL^{-1}, obvious current signal can be observed. The peak current density increases with the increase of *E. coli* O157:H7 concentration. As shown in Fig. 4**b**, The peak current density is linear with the common logarithm of *E. coli* O157:H7 concentration (*c*, CFU mL^{-1}) from 10 to 10^8 CFU mL^{-1}, with a linear regression equation of $\Delta j = 0.198 \times \log c - 0.164$ ($R^2 = 0.9987$). Note that here at low *E. coli* O157:H7 concentrations (< 10 CFU mL^{-1}), the peak current density is almost linear with *E. coli* O157:H7 concentration. The detection limit for our biosensor is 3 CFU mL^{-1} (S/N = 3). As listed in Table S1, the detection limits for electrochemical detection of *E. coli* O157:H7 reported previously are much higher than our value (typically higher than 30 CFU mL^{-1}). Moreover, our method is also more sensitive than other reported methods, including surface plasmon resonance, electrochemiluminescence, chemiluminescence, colorimetry, and fluorescence (Table S1).

An immunobiosensor was also fabricated using CdS QDs as signal tags. The fabrication steps were similar to those of the immunobiosensor using CdS@ZIF-8 as signal tags except that Ab-modified CdS QDs were used instead of CdS@ZIF-8@PEI-Ab. As shown in Fig. 4**c** and **d**, the linear range for *E. coli* O157:H7 detection is from 1×10^2 to 1×10^8 CFU mL^{-1}, with a linear regression equation of $\Delta j = 0.0123 \times \log c - 0.0227$ ($R^2 = 0.9983$). The detection limit of the immunobiosensor using CdS QDs as signal tags is 30 CFU mL^{-1} (S/N = 3), which is much higher than that of the immunobiosensor using CdS@ZIF-8 as signal tags. The sensitivity (slope of the regression curve) of the immunobiosensor using CdS@ZIF-8 as signal tags is 16 times that of the immunobiosensor using CdS QDs as signal tags. A great number of CdS QDs were encapsulated in each CdS@ZIF-8 label, so the number of CdS QDs labeled to each bacterial cell increased greatly. As a result, the DPV signals are amplified greatly by using CdS@ZIF-8 particles as signal tags.

The selectivity of the immunobiosensor using CdS@ZIF-8 as signal tags was studied. As shown in Fig. 5, the immunoelectrode shows a remarkable response to *E. coli* O157:H7, but shows negligible responses to other pathogens. These results indicate that the immunobiosensor has good selectivity toward the detection of *E. coli* O157:H7, resulting from the specific interactions between the *E. coli* O157:H7 Ab and surface antigen of *E. coli* O157:H7 cells.

To investigate the stability and reproducibility of the sensor, the detection of *E. coli* O157:H7 (1000 CFU mL^{-1}) was conducted every 3 day for 15 days using 6 different immunoelectrodes under the same conditions (Fig. S10a). We found that the relative standard deviations are below 5%, indicating that the sensor has good stability and reproducibility. The detection of *E. coli* O157:H7 in milks was carried out to study the application potential of the immunobiosensor (Fig. S10b). The milk samples were diluted with PBS for10 times, and we evaluated the recoveries by adding *E. coli* O157:H7 to the diluted milk samples. As shown in and Table 1, satisfactory recoveries (94.3–104.8%) were achieved, indicating that the proposed immunobiosensor is available for detecting *E. coli* O157:H7 in real samples.

4. Conclusions

In summary, CdS@ZIF-8 muti-core-shell particles were prepared by in situ growth of ZIF-8 in the presence of CdS QDs and used as signal-

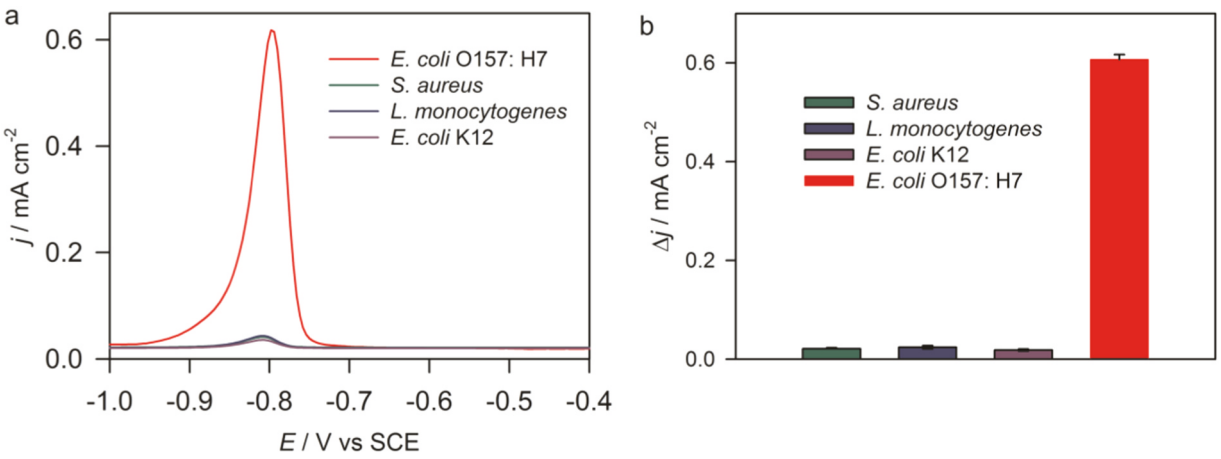

Fig. 5. Differential pulse voltammograms (a) and current responses (b) for the detection of various pathogens (10^4 CFU mL^{-1} for each).

Table 1
Results for determination of *E. coli* O157:H7 in milk samples.

Sample	Original (CFU mL^{-1})	Added (CFU mL^{-1})	Found (CFU mL^{-1})	Recovery (%)
Milk#1	Not found	1000	943 ± 5	94.3
		10,000	10,480 ± 10	104.8
		100,000	103,200 ± 10	103.2
Milk#2	Not found	1000	1030 ± 5	103
		10,000	9570 ± 10	95.7
		100,000	104,500 ± 10	104.5

amplifying tags for ultrasensitive electrochemical detection of *E. coli* O157:H7. Due to the great signal-amplifying effect, the sensitivity of the proposed immunobiosensor using CdS@ZIF-8 as signal tags was 16 times that of the conventional immunobiosensor using CdS QDs as signal tags. The detection limit for our biosensor is 3 CFU mL^{-1}, which is amongst the lowest reported in the literature. The developed immunobiosensor also showed good selectivity and was successfully used to detect *E. coli* O157:H7 in milk samples, indicating a promising method for sensitive electrochemical detection of pathogens. We believe that the signal-amplifying strategy can be extended to fabricate many other immunobiosensors.

Acknowledgment

This work was supported by the National Natural Science Foundation of China (21705045, 21305041, and 21475041), the Science and Technology Innovation Project of Hunan Province (2018RS3062), the Natural Science Foundation of Hunan Province (2018JJ2252), the Scientific Research Fund of Hunan Provincial Education Department (17A125), and the Science and Technology Project of Changsha (KQ1707009). M. Zhong and L.Yang contributed equally to this work.

Appendix A. Supplementary material

Supplementary data associated with this article can be found in the online version at doi:10.1016/j.bios.2018.11.001.

References

Aguilera-Sigalat, J., Bradshaw, D., 2016. Coord. Chem. Rev. 307, 267.
Alivisatos, A.P., 1996. Science 271, 933.
Alocilja, E.C., Radke, S.M., 2003. Biosens. Bioelectron. 18, 841.
Anderson, M.J., Miller, H.R., Alocilja, E.C., 2013. Biosens. Bioelectron. 42, 581.
Atrazhev, A., Manage, D.P., Stickel, A.J., Crabtree, H.J., Pilarski, L.M., Acker, J.P., 2010. Anal. Chem. 82, 8079.
Buso, D., Jasieniak, J., Lay, M.D.H., Schiavuta, P., Scopece, P., Laird, J., Amenitsch, H., Hill, A.J., Falcaro, P., 2012. Small 8, 80.
Charlermroj, R., Himananto, O., Seepiban, C., Kumpoosiri, M., Warin, N., Oplatowska, M., Gajanandana, O., Grant, I.R., Karoonuthaisiri, N., Elliott, C.T., 2013. PLoS One 8, e62344.
Chen, L., Luque, R., Li, Y., 2017. Chem. Soc. Rev. 46, 4614.
Deisingh, A.K., Thompson, M., 2004. J. Appl. Microbiol. 96, 419.
Dutta, R.K., Kumar, A., 2016. Anal. Chem. 88, 9071.
Esken, D., Turner, S., Wiktor, C., Kalidindi, S.B., Tendeloo, G.V., Fischer, R.A., 2011. J. Am. Chem. Soc. 133, 16370.
Fortin, N.Y., Mulchandani, A., Chen, W., 2001. Anal. Biochem. 289, 281.
Gayathri, C.H., Mayuri, P., Sankaran, K., Kumar, A.S., 2016. Biosens. Bioelectron. 82, 71.
He, M., Yao, J., Liu, Q., Wang, K., Chen, F., Wang, H., 2014. Microporous Mesoporous Mater. 184, 55.
Hildebrandt, N., Spillmann, C.M., Algar, W.R., Pons, T., Stewart, M.H., Oh, E., Susumu, K., Díaz, S.A., Delehanty, J.B., Medintz, I.L., 2017. Chem. Rev. 117, 536.
Hu, Y., Kazemian, H., Rohani, S., Huang, Y., Song, Y., 2011. Chem. Commun. 47, 12694.
Kokkinos, C., Angelopoulou, M., Economou, A., Prodromidis, M., Florou, A., Haasnoot, W., Petrou, P., Kakabakos, S., 2016. Anal. Chem. 88, 6897.
Lee, J., Farha, O.K., Roberts, J., Scheidt, K.A., Nguyen, S.T., Hupp, J.T., 2009. Chem. Soc. Rev. 38, 1450.
Ling, P., Lei, J., Zhang, L., Ju, H., 2015. Anal. Chem. 87, 3957.
Ma, W., Jiang, Q., Yu, P., Yang, L., Mao, L., 2013. Anal. Chem. 85, 7550.
Mao, X., Yang, L., Su, X.L., Li, Y., 2006. Biosens. Bioelectron. 21, 1178.
Mead, P.S., Slutsker, L., Dietz, V., McCaig, L.F., Bresee, J.S., Shapiro, C., Griffin, P.M., Tauxe, R.V., 1999. Emerg. Infect. Dis. 5, 607.
Michalet, X., Pinaud, F.F., Bentolila, L.A., Tsay, J.M., Doose, S., Li, J.J., Sundaresan, G., Wu, A.M., Gambhir, S.S., Weiss, S., 2005. Science 307, 538.
Qin, X., Xu, A., Liu, L., Deng, W., Chen, C., Tan, Y., Fu, Y., Xie, Q., Yao, S., 2015. Chem. Commun. 51, 8540.
Qin, X., Xu, A., Wang, L., Ling, L., Long, C., Fang, H., Tan, Y., Chao, C., Xie, Q., 2016. Biosens. Bioelectron. 79, 914.
Saha, S., Das, G., Thote, J., Banerjee, R., 2014. J. Am. Chem. Soc. 136, 14845.
Salam, F., Uludag, Y., Tothill, I.E., 2013. Talanta 115, 761.
Santos, M.B.D., Agusil, J.P., Prieto-Simón, B., Sporer, C., Teixeira, V., Samitier, J., 2013. Biosens. Bioelectron. 45, 174.
Setterington, E.B., Alocilja, E.C., 2011. Biosens. Bioelectron. 26, 2208.
Shen, W.J., Zhuo, Y., Chai, Y.Q., Yuan, R., 2015. Anal. Chem. 87, 11345.
Shen, Z., Huang, M., Xiao, C., Zhang, Y., Zeng, X., Wang, P.G., 2007. Anal. Chem. 79, 2312.
Su, X., Li, Y., 2004. Biosens. Bioelectron. 19, 563.
Sun, J., Ji, J., Sun, Y., Abdalhai, M.H., Zhang, Y., Sun, X., 2015. Biosens. Bioelectron. 70, 239.

Tan, J.C., Bennett, T.D., Cheetham, A.K., 2010. Proc. Natl. Acad. Sci. USA 107, 9938.
Thaitrong, N., Charlermroj, R., Himananto, O., Seepiban, C., Karoonuthaisiri, N., 2013. PLoS One 8, e83231.
Wang, D., Chen, J., Nugen, S.R., 2017a. Anal. Chem. 89, 1650.
Wang, S., Deng, W., Yang, L., Tan, Y., Xie, Q., Yao, S., 2017b. ACS Appl. Mater. Interfaces 9, 24440.
Wang, Z.Q., Cohen, S.M., 2009. Chem. Soc. Rev. 38, 1315.
Wu, S., Duan, N., Shi, Z., Fang, C., Wang, Z., 2014. Anal. Chem. 86, 3100.
Xu, M., Wang, R., Li, Y., 2017. Talanta 162, 511.
Yang, L., Deng, W., Cheng, C., Tan, Y., Xie, Q., Yao, S., 2018. ACS Appl. Mater. Interfaces 10, 3441.
Yang, L., Li, Y., Erf, G.F., 2004. Anal. Chem. 76, 1107.
Zhan, W., Kuang, Q., Zhou, J., Kong, X., Xie, Z., Zheng, L.S., 2013. J. Am. Chem. Soc. 135, 1926.
Zhang, X., Shen, J., Ma, H., Jiang, Y., Huang, C., Han, E., Yao, B., He, Y., 2016. Biosens. Bioelectron. 80, 666.
Zhu, Q.-L., Xu, Q., 2014. Chem. Soc. Rev. 43, 5468.